ARTICLE
PUBLISHED ONLINE: 1 FEBRUARY 2016 | DOI: 10.1038/NCHEMBIO.2017

Acetylation of Aurora B by TIP60 ensures accurate chromosomal segregation

Fei Mo[1,2,9], Xiaoxuan Zhuang[1,2,9], Xing Liu[1–5]*, Phil Y Yao[5], Bo Qin[1,2,5], Zeqi Su[5,6], Jianye Zang[1–4], Zhiyong Wang[1–4], Jiancun Zhang[1,2,7], Zhen Dou[1–4], Changlin Tian[1–4], Maikun Teng[1–4], Liwen Niu[1–4], Donald L Hill[8], Guowei Fang[1,2], Xia Ding[5,6], Chuanhai Fu[1–4] & Xuebiao Yao[1–4]*

Faithful segregation of chromosomes in mammalian cells requires bi-orientation of sister chromatids, which relies on the sensing of correct attachments between spindle microtubules and kinetochores. Although the mechanisms underlying cyclin-dependent kinase 1 (CDK1) activation, which triggers mitotic entry, have been extensively studied, the regulatory mechanisms that couple CDK1–cyclin B activity to chromosome stability are not well understood. Here, we identified a signaling axis in which Aurora B activity is modulated by CDK1–cyclin B via the acetyltransferase TIP60 in human cell division. CDK1–cyclin B phosphorylates Ser90 of TIP60, which elicits TIP60-dependent acetylation of Aurora B and promotes accurate chromosome segregation in mitosis. Mechanistically, TIP60 acetylation of Aurora B at Lys215 protects Aurora B's activation loop from dephosphorylation by the phosphatase PP2A to ensure a robust, error-free metaphase-anaphase transition. These findings delineate a conserved signaling cascade that integrates protein phosphorylation and acetylation with cell cycle progression for maintenance of genomic stability.

The maintenance of chromosome stability is pivotal for cellular homeostasis[1,2], wherein the sensing of genomic alterations represents a necessary step[3,4]. Several checkpoint pathways, such as the DNA damage response (DDR) and spindle assembly checkpoint (SAC) pathways, orchestrate cell cycle progression to provide quality control. Central to DDR signaling is the signaling cascade of the protein kinase ATM and the acetyltransferase TIP60 (Tat-interactive protein 60 kDa)[5]. Binding of TIP60 to Lys9-trimethylated histone H3 (H3K9me3) promotes TIP60-dependent activation of ATM[6]. Because H3K9me3 is also involved in centromere assembly and chromosome stability, and because some key components of DDR signaling, such as Chk1 (ref. 7), Chk2 (refs. 8,9) and BRCA1 (ref. 9), are essential for proper mitotic progression, how TIP60 functions at the centromere was regulated and whether it also guides chromosome dynamics and stability during mitosis have been outstanding questions.

Aurora B kinase is the catalytic subunit of the chromosome passenger complex (CPC), which localizes to inner centromeres in early mitosis and transfers to the central spindle upon metaphase-anaphase transition. The CPC complex governs chromosome segregation by generating spindle checkpoint signals and correcting aberrant kinetochore-microtubule attachments. Although inner-centromere localization of CPC also relies on post-translational modification of histone H3 tails, whether and how Aurora B and TIP60 cooperate in centromere was unclear.

Here, we identified a previously undefined regulatory mechanism underlying Aurora B kinase activation by TIP60 dependent acetylation. We found that TIP60 colocalizes with phosphorylated Aurora B at the outer kinetochore, where TIP60 directly acetylates Aurora B at Lys215, a process that is essential for Aurora B activation and chromosome bi-orientation. Biochemical characterization demonstrated that acetylation of Lys215 prevents PP2A dependent dephosphorylation of Aurora B at Thr232, thus sustaining a robust activity for correcting erroneous attachment. Interestingly, the CDK1–cyclin B complex phosphorylates TIP60 at Ser90, which promotes TIP60 activity at kinetochores and elicits TIP60-dependent acetylation of Aurora B. Our study has characterized a novel mechanism underlying CDK1–TIP60–Aurora B signaling axis that promotes accurate mitotic process and genomic stability.

RESULTS

TIP60 is essential for faithful chromosome segregation

To elucidate the function of TIP60 in mitosis, we employed two short hairpin RNAs (shRNAs) to suppress endogenous TIP60 (**Supplementary Results**, **Supplementary Fig. 1a**,**b**) in cultured human cells (HeLa cells, except as stated otherwise) and examined the resulting mitotic phenotype using time-lapse microscopy (**Fig. 1a** and **Supplementary Fig. 1c**). Whereas cells treated with control shRNA progressed normally through mitosis, TIP60-depleted cells showed a high frequency of chromosome segregation defects, including anaphase lagging chromosomes, chromosome misalignment and chromosome bridges (**Fig. 1b–d**). The defects seen in the TIP60-deficient cells were largely rescued by expressing an RNA interference (RNAi)-resistant, wild-type TIP60, but not with an acetyltransferase-deficient form of TIP60 (ref. 10) (**Supplementary Fig. 1d–g**), demonstrating the role of TIP60 acetyltransferase activity in mitotic chromosome movements. To eliminate the possibility that the phenotype was a consequence of disruption of TIP60 function in the DDR pathway, we introduced two small-molecule inhibitors of TIP60 acetyltransferase (NU9056 and MG149; refs. 11,12) into cultured cells immediately after mitotic entry. As expected, TIP60 acetyltransferase activity inhibition in mitosis resulted in increased rates of chromosome mis-segregation (**Fig. 1e–g** and **Supplementary Fig. 1h**). Thus, TIP60 acetyltransferase activity

[1]Anhui Key Laboratory for Cellular Dynamics & Chemical Biology, Hefei, China. [2]Laboratory for Organelle Dynamics & Plasticity Control, University of Science & Technology of China School of Life Sciences, Hefei, China. [3]Chinese Academy of Sciences Center for Excellence in Molecular Cell Science, Hefei, China. [4]Hefei National Laboratory for Physical Sciences at Nanoscale, Hefei, China. [5]Molecular Imaging Center, Morehouse School of Medicine, Atlanta, Georgia, USA. [6]Department of Medical Cell Biology, Beijing University of Chinese Medicine, Beijing, China. [7]State Key Laboratory of Respiratory Diseases, Guangzhou, China. [8]Comprehensive Cancer Center, University of Alabama, Birmingham, Alabama, USA. [9]These authors contributed equally to this work. *e-mail: yaoxb@ustc.edu.cn or xing1017@ustc.edu.cn

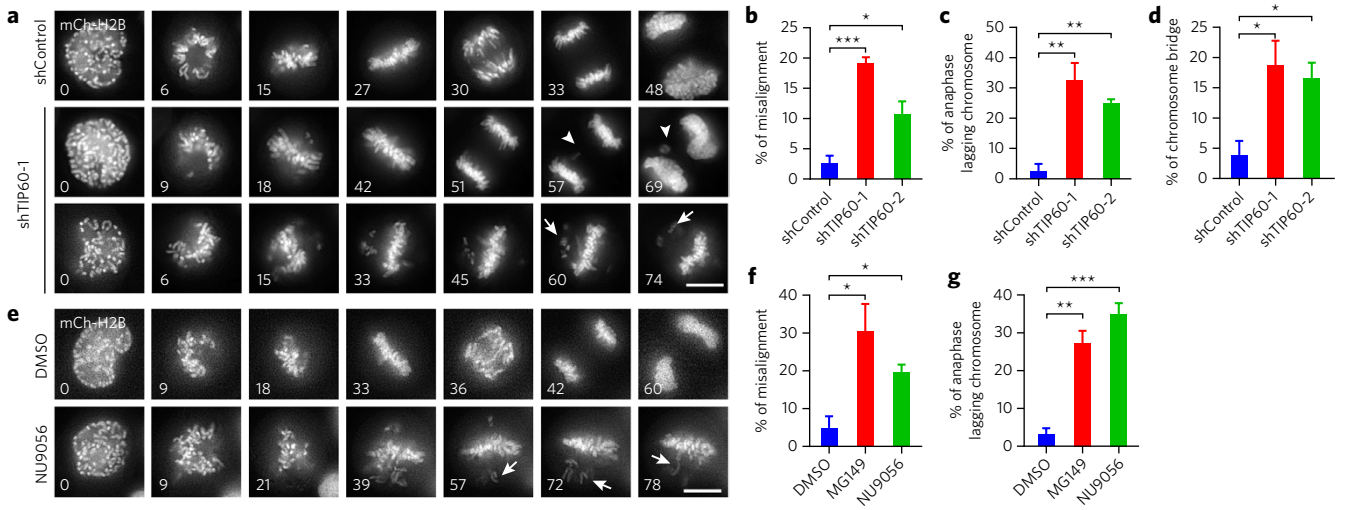

Figure 1 | Accurate chromosome segregation in mitosis requires TIP60 acetyltransferase activity. (**a**) Representative mitotic phenotypes in HeLa cells expressing shTIP60-1 or control shRNA shown by time-lapse microscopy, visualized with mCherry-H2B (mCh-H2B) (arrowheads, lagging chromosomes; arrows, misalignment; numbers at bottom left of images indicate elapsed time in minutes). (**b**–**d**) Quantification of chromosome segregation defects of live HeLa cells expressing control (n = 108) or TIP60 shRNA (n = 129, shTIP60-1; n = 104, shTIP60-2). Cells exhibiting unaligned chromosomes and failing to align at the metaphase plate within 60 min after nuclear envelope breakdown were considered to be misaligned (**b**). Data represent mean ± s.e.m. from three independent experiments. (**e**) Representative phenotypes in HeLa cells treated with DMSO or with the TIP60 inhibitor NU9056 immediately after mitotic entry (arrows, misalignment; ACA, anti-centromere antibodies). (**f**,**g**) Quantification of mitotic phenotypes of live HeLa cells treated with DMSO (n = 103), NU9056 (n = 101) or MG149 (n = 105) immediately after mitotic entry. Data represent mean ± s.e.m. from three independent experiments. Statistical significance was tested by two-sided t-test; $^{*}P < 0.05$, $^{**}P < 0.01$, $^{***}P < 0.001$. Scale bars, 5 μm.

was essential for chromosome alignment and accurate metaphase-anaphase transition. The function of TIP60 in genomic stability was apparent, as suppression of TIP60 gave rise to micronuclei and polyploidy (**Supplementary Fig. 1i**–**k**).

TIP60 modulates Aurora B kinase activity at kinetochores

To delineate the mechanism of action underlying TIP60 function in mitosis, we examined the subcellular distribution of TIP60 during this process. Consistent with its function, TIP60 localized to kinetochores in early mitosis, as determined with two different TIP60 antibodies (**Fig. 2a** and **Supplementary Fig. 2a**). The localization of TIP60 to kinetochores was independent of microtubules, as nocodazole treatment did not alter its localization (**Supplementary Fig. 2b**). In a line scan, the fluorescence intensity profiles suggested that TIP60 colocalized with Hec1 at the outer kinetochores (**Fig. 2b** and **Supplementary Fig. 2c**). The kinetochore localization of TIP60 was abolished by shRNA-mediated suppression, confirming the specificity of the antibody (**Supplementary Fig. 2d**). Furthermore, exogenously expressed TIP60-GFP also localized to the kinetochores in prometaphase cells (**Supplementary Fig. 2e**), confirming that TIP60 is a kinetochore protein.

The localization of TIP60 prompted us to search, with a battery of kinase inhibitors, for the molecular determinants underlying its localization; the results indicated that a stable localization of TIP60 to the kinetochores specifically requires Mps1 kinase activity (**Supplementary Fig. 3a**–**c**). The Mps1 dependence was confirmed by short interfering RNA (siRNA) treatment in which suppression of Mps1 quantitatively reduced the levels of TIP60 at the kinetochores (**Supplementary Fig. 3d**). We and two other groups have recently found that Mps1 is recruited to kinetochores by binding to two distinct areas of the Ndc80 complex[13–15]. To determine whether kinetochore recruitment of TIP60 required adequate Mps1 kinase at kinetochores, we knocked down two components of the Ndc80 complex, Hec1 and Nuf2. The absence of either Nuf2 or Hec1 abolished kinetochore localization of TIP60 (**Supplementary Fig. 3e**), confirming that the Ndc80-Mps1 pathway regulated TIP60 distribution to kinetochore[16].

Because TIP60 transiently localized to kinetochores in early mitosis when chromosomes attempted bi-orientation, we questioned whether TIP60 distinguished amphitelic attachment from erroneous attachment of kinetochores. To this end, we treated HeLa cells with the mitotic kinesin CENP-E inhibitor GSK923295 (IC_{50} = 3.2 nM)[17] to create erroneous kinetochore-microtubule attachments. TIP60 preferentially accumulated at erroneously attached kinetochores near the spindle poles but not at those with apparent amphitelic attachments (**Supplementary Fig. 3f**). Quantitative analyses of normalized pixel intensities indicated that the level of kinetochore-associated TIP60 was a function of chromosome position with respect to the poles (**Fig. 2c**). We next further assessed the function of TIP60 in chromosome alignment. In a monastrol washout assay, bi-orientation was achieved only after either of the TIP60 inhibitors was removed (**Supplementary Fig. 4a**). Consistently, TIP60-depleted cells also failed to undergo accurate chromosome segregation, as lagging chromosomes were frequently observed (**Supplementary Fig. 4b**), confirming that the achievement of chromosome bi-orientation required TIP60 activity. Because Aurora B kinase is a key factor in correcting erroneous attachments[18,19], we sought to examine whether the function of TIP60 in promoting accurate kinetochore attachment was mediated via Aurora B signaling. To this end, we depleted Aurora B through siRNA treatment. Although Aurora B depletion caused a more severe phenotype than did TIP60 depletion, there was no additive effect when Aurora B and TIP60 were depleted in combination (**Supplementary Fig. 4c**,**d**), revealing that there is a functional relationship between the two proteins. Because an active form of Aurora B (Thr232 phosphorylated) localizes to kinetochores[20], where it colocalized with TIP60 (**Fig. 2d**), we further examined the intensity of Thr232-phosphorylated Aurora B in TIP60-depleted cells (**Fig. 2e**). Quantitative analysis showed that the abundance of pT232 in TIP60 siRNA–treated cells was

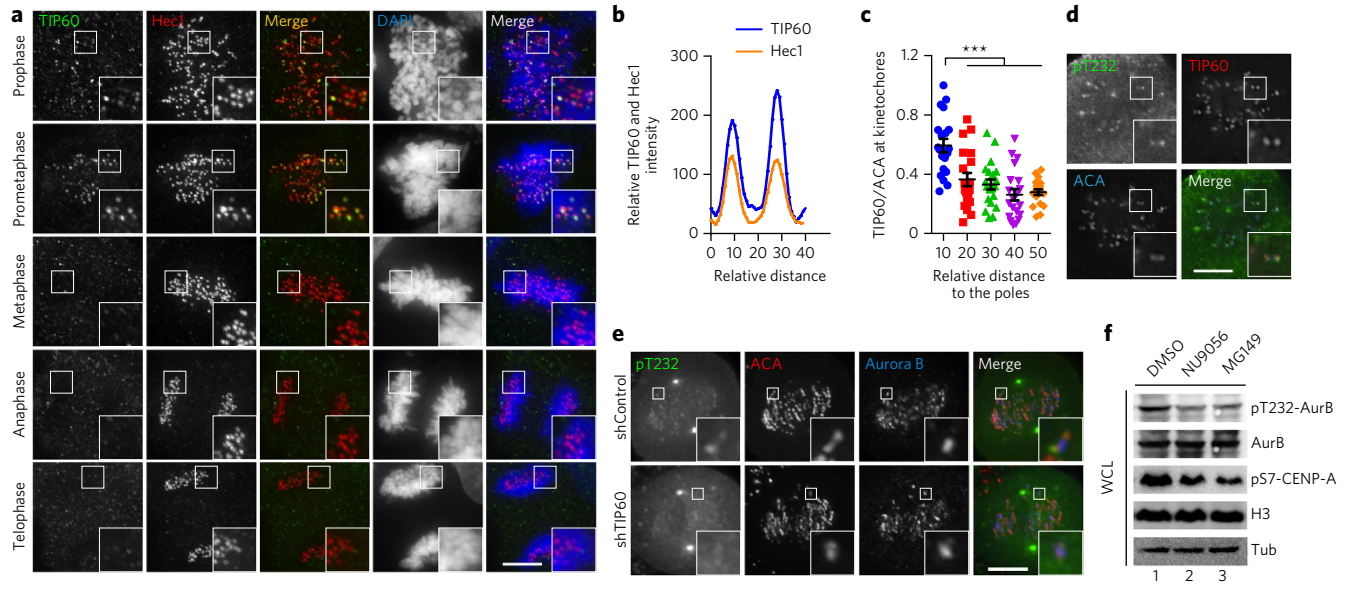

Figure 2 | TIP60 localizes to kinetochores and orchestrates accurate kinetochore-microtubule attachments. (**a**) Immunofluorescence staining of TIP60 and Hec1 in HeLa cells from different mitotic stages. (**b**) Plot profile of TIP60 and Hec1 fluorescence intensity across the kinetochore pair. See also **Supplementary Figure 2c**. (**c**) Quantification of TIP60 fluorescence intensity (normalized to ACA) at kinetochores relative to the distance from the spindle poles in GSK923295-treated cells. Data represent mean ± s.e.m. and were examined with two-sided *t*-test. A total of 100 kinetochores were examined from three independent experiments. (**d**) Colocalization analysis of TIP60 and Thr232-phosphorylated Aurora B (pT232) at prometaphase kinetochores in HeLa cells. (**e**) HeLa cells expressing control or TIP60 shRNA were fixed and stained for the indicated antibody as illustrated. (**f**) Mitotic HeLa cells were shaken off and treated with DMSO, NU9056 (20 μM) or MG149 (100 μM) for 1 h in the presence of MG132 before harvest. Whole-cell lysates (WCL) were separated by SDS-PAGE and blotted with the indicated antibodies to examine Aurora B kinase activity. See also **Supplementary Figure 9**. Statistical significance was tested by two-sided *t*-test; ***$P < 0.001$. Scale bars, 5 μm.

reduced to 33% of the value in control siRNA–treated cells, whereas average Aurora B protein levels were not significantly altered (**Supplementary Fig. 4e,f**), suggesting that TIP60 regulated the activity of kinetochore-bound Aurora B.

To probe whether Aurora B kinase activity is modulated by TIP60-mediated acetylation, we examined Aurora B activity using phosphorylation of CENP-A (a cognate substrate of Aurora B that localizes constitutively to kinetochores) at Ser7 (pS7-CENP-A) as a reporter[21]. Suppressing TIP60 acetyltransferase activity with either TIP60 inhibitors (**Fig. 2f**) or TIP60 shRNA (**Supplementary Fig. 4g,h**) reduced CENP-A phosphorylation, suggesting that TIP60-mediated acetylation modulated Aurora B kinase activity in mitotic cells. The effect of TIP60 inhibition on Aurora B activation, together with the colocalization of phosphorylated Aurora B and TIP60, prompted us to investigate whether TIP60 formed a complex with Aurora B *in vivo*. In mitosis, gel filtration assays and reciprocal co-immunoprecipitation confirmed that TIP60 formed a complex with Aurora B (**Supplementary Fig. 5a–c**). Thus, we concluded that TIP60 acetyltransferase modulates Aurora B kinase activity in mitosis.

Lys215 acetylation by TIP60 promotes Aurora B activity

We next addressed whether TIP60 directly acetylates Aurora B. Western blots with antibody to pan-acetyllysine (acK) established that Aurora B was a substrate of TIP60 *in vitro* (**Fig. 3a**). To identify the physiological substrate sites of TIP60 in Aurora B, we subjected purified Aurora B from mitotic HeLa cells to MS analyses, which revealed four potential acetylation sites: Lys31, Lys115, Lys215 and Lys231 (**Supplementary Fig. 5d**). To map the site(s) responsible for TIP60 acetylation, we generated a series of Aurora B mutants in which the identified acetylation sites were individually mutated to arginine. In the Aurora B Lys215 mutant K215R immunoprecipitated from mitotic cells, Aurora B acetylation was virtually undetectable (**Supplementary Fig. 5e**), suggesting that K215ac accounted for Aurora B acetylation in mitosis. To characterize the precise cellular function of Lys215 acetylation in mitosis, we generated an antibody to K215ac Aurora B, which specifically recognized both endogenous acetylated Aurora B (**Supplementary Fig. 5f,g**) and TIP60-acetylated Aurora B *in vitro* (**Supplementary Fig. 5h**). To assess whether Aurora B is a cognate substrate of TIP60 in mitosis, we analyzed Lys215 acetylation in aliquots of unsynchronized or nocodazole-synchronized HeLa cells. Lys215 acetylation was dramatically increased in nocodazole-synchronized cells but reduced after TIP60 inhibition (**Supplementary Fig. 5i**), indicating that Lys215 is a cognate substrate of TIP60 in mitotic cells. To examine the precise cellular function of Lys215 acetylation by TIP60, we knocked down endogenous TIP60 and assessed the activity of Aurora B by *in vitro* kinase assays. Aurora B kinase activity was alleviated in TIP60-depleted cells, consistent with the reduced Lys215 acetylation level (**Fig. 3b**), indicating that both Lys215 acetylation and kinase activity of Aurora B require TIP60.

Because Lys215 is highly conserved among species and locates close to the activation loop of Aurora B (**Supplementary Fig. 5j**), we hypothesized that TIP60 promotes Aurora B activity by acetylating Aurora B at Lys215. To confirm the hypothesis, we purified FLAG-tagged wild-type (WT) Aurora B and acetylation-mimicking (K215A) and non-acetylatable (K215R) mutants from mitotic cells for *in vitro* kinase assay and enzymatic characterization. As reflected by H3 phosphorylation, TIP60-mediated K215 acetylation robustly stimulated Aurora B activity (**Fig. 3c,d** and **Supplementary Fig. 5k**).

Lys215 acetylation promotes chromosome bi-orientation

Since TIP60 distinguished bi-oriented kinetochores from erroneously attached kinetochores, we next tested whether altering the kinetochore-microtubule attachment modulated distribution of acetylated Aurora B at the kinetochores. K215ac staining was apparent in prometaphase, when bi-orientation was not achieved in most kinetochores, but was diminished in metaphase, when

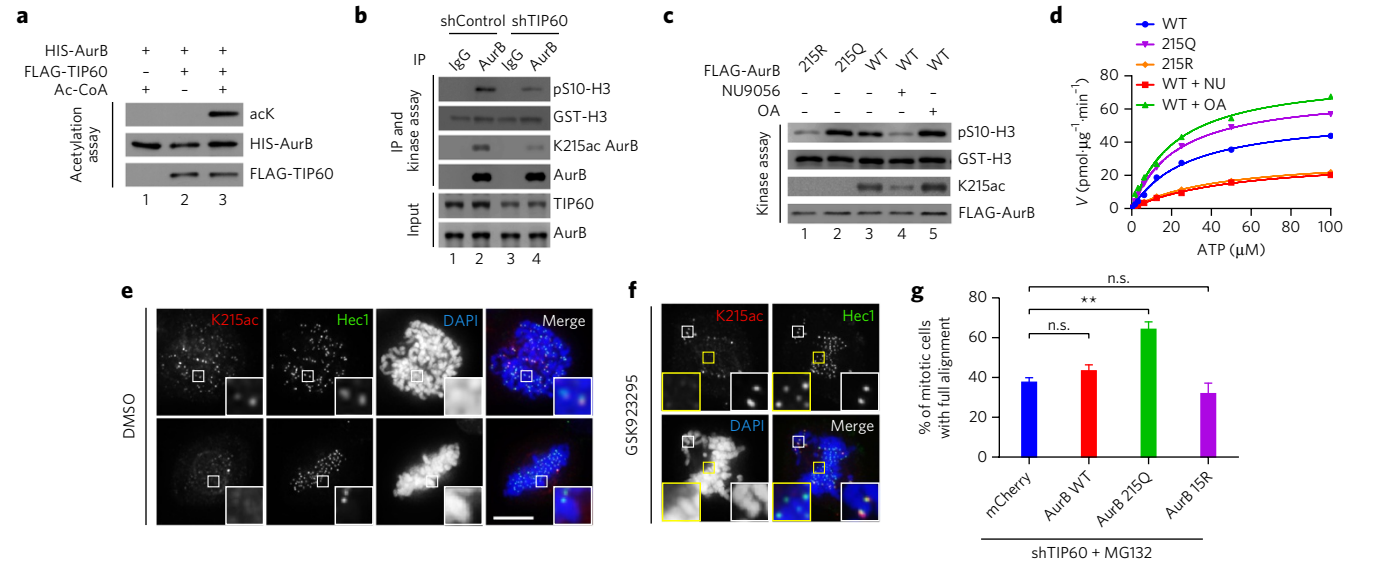

Figure 3 | Acetylation of Aurora B by TIP60 promotes Aurora B kinase activity and attachment error correction. (**a**) FLAG-TIP60 was incubated with 6xHIS tagged Aurora B (HIS-AurB) in the presence of Ac-CoA for *in vitro* acetylation assay. The acetylation levels of Aurora B were analyzed with an anti-acetyllysine antibody (acK). (**b**) HeLa cells expressing control or TIP60 shRNA were subjected to immunoprecipitation with Aurora B antibody or IgG. The activity of immunoprecipitated Aurora B was measured by *in vitro* phosphorylation. (**c**) HeLa cells expressing FLAG-conjugated wild-type (WT) and Lys215 mutant (K215R (215R) and K215Q (215Q)) Aurora B were synchronized by nocodazole treatment (100 ng/mL), and the indicated inhibitors (NU9056 or okadaic acid, OA) were added for 0.5 h in the presence of MG132. Immunoisolated Aurora B was subjected to an *in vitro* kinase assay with GST-H3. (**d**) Kinetics curves of Aurora B (purified as in **c**) generated by a fluorometry-based kinase assay. (**e**) Immunofluorescence staining of K215ac and Hec1 in DMSO-treated prometaphase or metaphase HeLa cells. (**f**) Immunofluorescence staining of K215ac and Hec1 in GSK923295-treated HeLa cells. Note that GSK923295 produced aligned (yellow) and unaligned kinetochores (white) in the same cell. (**g**) Phenotypes of fixed TIP60-depleted cells expressing mCherry or wild-type (AurB WT), K215Q (AurB K215Q) or K215R Aurora B (AurB K215R). At least 108 cells per group (n = 108, mCherry; n = 115, AurB WT; n = 114, AurB K215Q; n = 108, AurB K215R) were examined from three independent experiments. Data represent mean ± s.e.m. and were examined with two-sided t-test. $^{**}P < 0.01$; n.s. (nonsignificant) indicates $P > 0.05$. Scale bar, 5 μm (same scale is used in **e** and **f**). See also **Supplementary Figure 9**.

most kinetochores were properly attached to microtubules (**Fig. 3e** and **Supplementary Fig. 6a**).

If acetylation of Lys215 was involved in the correction of aberrant kinetochore attachments, the level of K215ac would increase in misaligned kinetochores. To test this hypothesis, we exposed HeLa cells to GSK923295 to create both bi-oriented and misaligned kinetochores in the same cell, and found that the labeling of K215ac was brighter on the misaligned kinetochores (**Fig. 3f**). Statistical analysis indicated that K215ac levels of misaligned kinetochores were about six-fold higher than those near the equator (**Supplementary Fig. 6a**). We also examined the levels of pT232, a reporter of Aurora B activity, in GSK923295-treated cells and found that these were

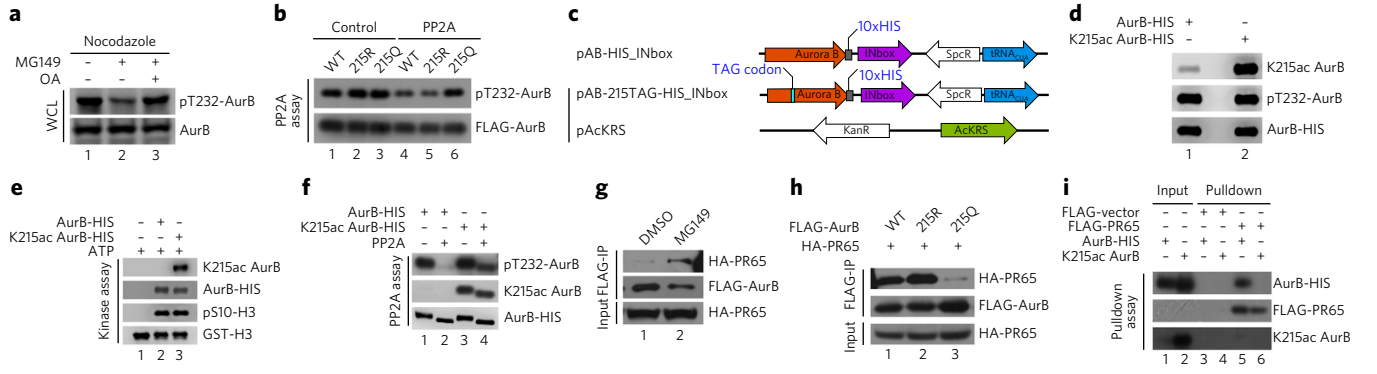

Figure 4 | Acetylation of Aurora B by TIP60 antagonizes dephosphorylation of Thr232 by PP2A. (**a**) Nocodazole-arrested HeLa cells were treated with MG149 (100 μM) or MG149 plus okadaic acid (OA; 500 nM), and the Aurora B phosphorylation levels in whole-cell lysates (WCL) were assessed by western blotting. (**b**) FLAG-tagged Aurora B was purified from lysates of OA (500 nM)-treated mitotic HeLa cells and incubated with PP2A phosphatase for 30 min. The reaction was then analyzed by western blotting. (**c**) Diagram of plasmid combinations used to produce recombinant K215ac or wild-type Aurora B in *E. coli*. (**d**) Purified wild-type and K215ac Aurora B were analyzed by western blotting using antibodies to K215ac and to pT232, respectively. (**e**) Wild-type and K215ac Aurora B were subjected to *in vitro* phosphorylation using GST-H3 as substrate. (**f**) Recombinant Aurora B and K215ac Aurora B were incubated with PP2A phosphatase for 2 h, and their phosphorylation levels were assessed by western blotting. (**g**) HeLa cells coexpressing FLAG–Aurora B and HA-PR65 were treated with DMSO or MG149 (100 μM) for 30 min, subjected to anti-FLAG resin immunoprecipitation and analyzed by western blotting. (**h**) FLAG–Aurora B wild-type and Lys215 mutant were co-transfected with HA-PR65 in HeLa cells, and their interactions were tested by co-immunoprecipitation. (**i**) FLAG-resin captured PR65 was incubated with recombinant Aurora B or K215ac Aurora B. The binding fractions were analyzed by western blotting. See also **Supplementary Figure 9**.

elevated in the kinetochores near the pole relative to kinetochores near the equator (**Supplementary Fig. 6b**). Statistical analyses showed that the pT232–Aurora B levels of misaligned kinetochores were much higher than those near the equator (**Supplementary Fig. 6c**), supporting the notion that K215ac promotes Aurora B activity at misattached and unattached kinetochores. Intriguingly, a brief treatment with the TIP60 inhibitor NU9056 abolished the labeling of K215ac and pT232 at the misaligned kinetochores (**Supplementary Fig. 6d,e**), indicating that TIP60 regulated Aurora B acetylation and activity on these kinetochores. If elevated acetylation of Aurora B by TIP60 were necessary for chromosome bi-orientation, introduction of the acetylation-mimicking K215Q Aurora B would partially reverse the chromosome misalignment seen in TIP60-depleted cells. Indeed, expression of acetylation-mimicking K215Q Aurora B, but not wild-type or non-acetylatable K215R, partially rescued the chromosome alignment in TIP60-depleted cells (**Fig. 3g** and **Supplementary Fig. 6f**). Thus, we concluded that Aurora B kinase activity is modulated by acetylation in mitosis and that TIP60-dependent acetylation of Aurora B at the kinetochores promotes chromosome bi-orientation.

K215 acetylation prevents PP2A-mediated inactivation

Because inhibition of TIP60 led to dephosphorylation of pT232, an autophosphorylation site essential for Aurora B activity[22] and a substrate of PP2A phosphatase[23], we next determined whether acetylation of Lys215 promoted phosphorylation of Thr232 through antagonizing PP2A function. In TIP60-inhibited cells, the reduction of pT232 was partially reversed by treatment with okadaic acid (OA), which preferentially inhibits PP2A at lower concentration[24,25] (**Fig. 4a**). To determine whether K215ac Aurora B prevented PP2A-elicited dephosphorylation of pT232, we conducted an *in vitro* PP2A assay in which the K215Q mutant attenuated the PP2A-mediated dephosphorylation of Thr232 (**Fig. 4b**). To directly determine whether Lys215 acetylation antagonized PP2A-mediated dephosphorylation of Thr232, we took advantage of a recently developed, genetically encoded method to obtain K215ac Aurora B[26,27] and a truncated version (residues 822–918) of INCENP (a binding partner that promotes the autocatalytic phosphorylation of Aurora B at Thr232)[28,29] from *Escherichia coli* (**Fig. 4c** and **Supplementary Fig. 7a,b**). Wild-type and acetylated Aurora B exhibited comparable Thr232 phosphorylation, but the anti-K215ac antibody specifically recognized the latter (**Fig. 4d**). Although K215ac Aurora B did not show greater activity than wild-type Aurora B, as determined by an *in vitro* kinase assay (**Fig. 4e**), Thr232 phosphorylation was largely preserved after incubation with PP2A phosphatase for 2 h (**Fig. 4f**), supporting the notion that Lys215 acetylation promoted Aurora B activity through antagonizing PP2A-mediated dephosphorylation.

Furthermore, suppression of TIP60 with MG149 preserved the Aurora B–PP2A interaction *in vivo* (**Fig. 4g**). Consistently with this, the Aurora B K215Q mutant that mimicked acetylation also failed to bind PP2A, as determined by a co-immunoprecipitation assay (**Fig. 4h**). This acetylation-elicited perturbation of the Aurora B–PP2A interaction was confirmed by a pulldown assay in which FLAG-PR65 interacted with wild-type Aurora B rather than with Lys215-acetylated Aurora B (**Fig. 4i**). Thus, the acetylation of

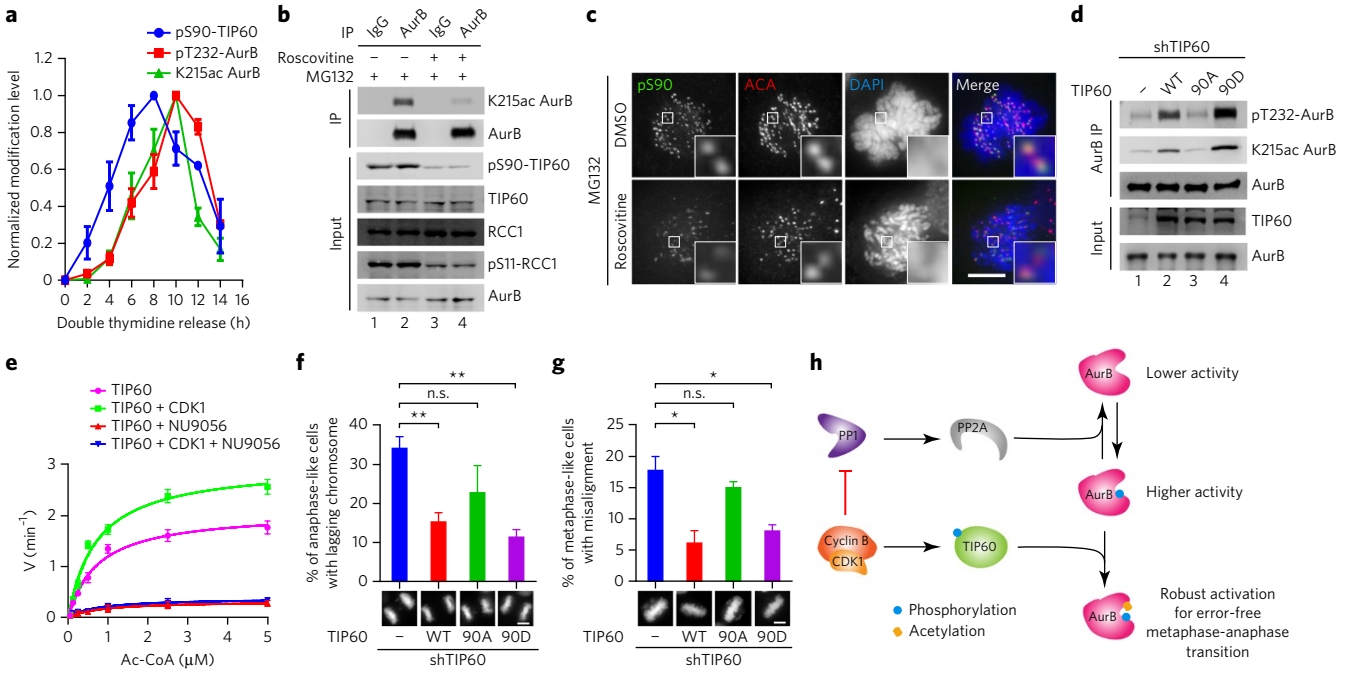

Figure 5 | Phosphorylation of TIP60 by CDK1 promotes Aurora B activity for error-free chromosome segregation. (**a**) Temporal profile of cyclin B accumulation, TIP60 phosphorylation and Aurora B acetylation. Data represent mean ± s.e.m. from three independent analyses. (**b**) Nocodazole-synchronized HeLa cells were treated with DMSO or roscovitine (20 μM) in the presence of MG132 (10 μM) for 20 min. Aurora B was immunoprecipitated and analyzed with the indicated antibodies. (**c**) HeLa cells treated with MG132 plus DMSO or roscovitine were fixed and immunostained with TIP60-pS90 antibody and ACA, respectively. (**d**) FLAG-tagged wild-type TIP60 and TIP60 mutants were expressed in TIP60-depleted HeLa cells. Aurora B was immunoprecipitated to test levels of Lys215 acetylation and Thr232 phosphorylation. (**e**) The kinetics curves of TIP60 acetyltransferase activity were measured using [^{14}C]Ac-CoA at various concentrations. FLAG-TIP60 was purified from HEK293T cells and then subjected to CDK1 phosphorylation on beads before the acetyltransferase assay. NU9056 was used at 10 μM for 10 min before acetyltransferase assay. Data represent mean ± s.e.m. from three independent analyses. (**f**,**g**) TIP60-depleted cells were co-transfected with ten-fold higher amount of TIP60 wild type or mutants along with mCherry-H2B. Phenotypes of fixed cells were determined under a microscope. Representative phenotypes of each group were shown at the bottom (n = 100 for each group). (**h**) Model for CDK1–TIP60–Aurora B signaling axis. All data were examined with two-sided t-test; *P < 0.05, ** P < 0.01 and n .s. (nonsignificant) indicates P > 0.05. Scale bars, 5 μm. See also **Supplementary Figure 9**.

Lys215 by TIP60 sustains Aurora B activity by protecting pT232 from PP2A-elicited dephosphorylation.

CDK1 phosphorylates TIP60 to ensure accurate mitosis

The phosphorylation of TIP60 at Ser90 by CDK1 has been reported[30–32]. To assess the spatiotemporal dynamics of CDK1-elicited phosphorylation of TIP60 and delineate its relevance in mitosis, we generated a phospho-Ser90–specific antibody (pS90), which specifically recognized phosphorylated TIP60 both *in vivo* and *in vitro* (**Supplementary Fig. 8a**,**b**). We next determined the temporal dynamics of pS90-TIP60 levels relative to those of K215ac Aurora B during mitosis by collecting synchronized HeLa cells at indicated intervals after release from the G1/S phase for immunoprecipitation assays (**Fig. 5a** and **Supplementary Fig. 8c**). The temporal dynamics of pS90 were similar to those of cyclin B, suggesting that TIP60 was temporally regulated by CDK1–cyclin B1. Furthermore, pT232–Aurora B and pS7-CENP-A levels in cells correlated with K215ac variation, and were parallel to those of pS90 with a brief lag, suggesting that Aurora B activity was tightly regulated by TIP60-S90 phosphorylation and TIP60-dependent Aurora B Lys215 acetylation. Levels of pS90 and K215ac were increased by nocodazole treatment (**Supplementary Fig. 8c**) but were diminished upon inhibition of CDK1 by roscovitine (**Fig. 5b**, combined with MG132 to prevent cyclin B degradation; treatment was also limited to 20 min to prevent mitotic exit[33]); this suggested that CDK1 kinase activity controlled TIP60-dependent modulation of Aurora B activity. Furthermore, an immunofluorescence assay showed that CDK1 inhibition abolished the pS90 signal at kinetochores in mitotic cells, indicating that pS90 is a substrate of CDK1 during mitosis (**Fig. 5c** and **Supplementary Fig. 8d**). In TIP60-depleted cells, either wild-type or S90D mutant TIP60, but not the S90A mutant, restored Lys215 acetylation and T232 phosphorylation of Aurora B, suggesting that robust TIP60 activation in mitosis required CDK1-dependent S90 phosphorylation (**Fig. 5d**).

We also evaluated TIP60 acetyltransferase activity through an *in vitro* assay using ^{14}C-labeled acetyl coenzyme A ([^{14}C]Ac-CoA) as the acetyl donor. The acetyltransferase activity was increased by CDK1 phosphorylation but diminished after addition of NU9056, a specific inhibitor of TIP60 (**Fig. 5e** and **Supplementary Fig. 8e**), confirming a direct function of CDK1–cyclin B in promoting TIP60 activity via phosphorylation of S90. If elevated phosphorylation of TIP60 by CDK1 were necessary for accurate chromosome segregation, introduction of the phosphorylation-mimicking S90D-TIP60 should reverse the chromosome segregation errors seen in TIP60-suppressed cells. As predicted, expression of the nonphosphorylatable S90A mutant failed to rescue Aurora B activity or correct chromosome segregation errors (**Fig. 5f**,**g**), revealing a temporal coordination of the CDK1–TIP60–Aurora B signaling axis in linking cell cycle progression to maintenance of genomic stability. Additional experiments to address whether Mps1 would synergize with CDK1 in release of TIP60 from the kinetochores in the presence of MG132 demonstrated that simultaneous inhibition of CDK1 and Mps1 did not result in any additive effects on TIP60 delocalization (**Supplementary Fig. 8f**,**g**). Thus, we concluded that CDK1-elicited phosphorylation of TIP60 promotes the correction of attachment errors in mitosis via acetylation and activation of Aurora B at the kinetochores.

DISCUSSION

Kinetochores are specialized protein machines involved in maintaining genome stability during mitosis by orchestrating accurate chromosome-microtubule attachments and SAC[34]. CDK1–cyclin B inhibits PP1 activity in early mitosis, and reduction of cyclin B levels later in mitosis permit PP1 autoreactivation, which reactivates PP2A for subsequent dephosphorylation of Aurora B at Thr232 (ref. 35). Acetylation of Aurora B by TIP60 therefore provided full activity of Aurora B for optimal correction of errors in kinetochore attachment before sister chromatid separation. Our identification of the CDK1–TIP60–Aurora B signaling axis uncovered a new regulatory mechanism by which acetylation of Aurora B prevented PP2A-mediated dephosphorylation of T-loops to enhance the activity of Aurora B for control of genomic stability (**Fig. 5h**). It would be of great interest, in follow-up studies, to characterize additional substrates of TIP60 in mitotic cells and delineate their precise molecular function in mitosis.

We identified a mechanism involving the CDK1–TIP60–Aurora B axis that underlies kinetochore sensing of aberrant microtubule attachment and established its connection to error-free metaphase-anaphase transition, as perturbation of the axis gave rise to polyploidy or micronuclei, characteristics of genomic instability[36]. This highlighted how an acetylation-phosphorylation cascade in the sensing and correction of chromosome attachment errors during mitotic progression maintains genomic stability. Alterations in chromatin promote TIP60 binding to chromatin and the concurrent accumulation of tyrosine phosphorylation of TIP60, which in turn induces ATM-mediated signaling and DNA damage checkpoint activation[37]. Of note, the control of centromere plasticity shares common machinery with the DDR, such as the MHF–CENP-X complex[38,39]. Indeed, chromosome segregation errors cause DNA damage and structural chromosome aberrations[40]. Our present study delineates the cellular function of TIP60 in mitosis but not earlier events by which CDK1-elicited activation of TIP60 orchestrated acetylation of Aurora B at the kinetochores for accurate chromosome alignment and segregation. These results explain how TIP60 serves as a genome guardian by orchestrating chromatin plasticity during DDR processes and generating an optimal Aurora B activity for kinetochore attachment and error-free metaphase-anaphase transition in mitosis (**Fig. 5h**).

Together with our findings that PCAF-mediated acetylation controls microtubule plus-end dynamics[41] and synergism between TIP60 and PCAF[42], this work provides a unifying view of a previously uncharacterized molecular mechanism that underlies acetyl regulation in mitosis and defines a signaling axis that integrates protein phosphorylation and acetylation to connect cell cycle progression with genomic stability.

Received 8 September 2015; accepted 11 December 2015; published online 1 February 2016

METHODS

Methods and any associated references are available in the online version of the paper.

References

1. Cleveland, D.W., Mao, Y. & Sullivan, K.F. Centromeres and kinetochores: from epigenetics to mitotic checkpoint signaling. *Cell* **112**, 407–421 (2003).
2. Kabeche, L. & Compton, D.A. Cyclin A regulates kinetochore microtubules to promote faithful chromosome segregation. *Nature* **502**, 110–113 (2013).
3. Orthwein, A. *et al.* Mitosis inhibits DNA double-strand break repair to guard against telomere fusions. *Science* **344**, 189–193 (2014).
4. Jackson, S.P. & Bartek, J. The DNA-damage response in human biology and disease. *Nature* **461**, 1071–1078 (2009).
5. Lee, J.H. & Paull, T.T. Direct activation of the ATM protein kinase by the Mre11/Rad50/Nbs1 complex. *Science* **304**, 93–96 (2004).
6. Sun, Y. *et al.* Histone H3 methylation links DNA damage detection to activation of the tumour suppressor Tip60. *Nat. Cell Biol.* **11**, 1376–1382 (2009).
7. Zachos, G. *et al.* Chk1 is required for spindle checkpoint function. *Dev. Cell* **12**, 247–260 (2007).
8. Petsalaki, E. & Zachos, G. Chk2 prevents mitotic exit when the majority of kinetochores are unattached. *J. Cell Biol.* **205**, 339–356 (2014).
9. Stolz, A. *et al.* The CHK2-BRCA1 tumour suppressor pathway ensures chromosomal stability in human somatic cells. *Nat. Cell Biol.* **12**, 492–499 (2010).
10. Cheng, Z. *et al.* Functional characterization of TIP60 sumoylation in UV-irradiated DNA damage response. *Oncogene* **27**, 931–941 (2008).

11. Coffey, K. *et al.* Characterisation of a Tip60 specific inhibitor, NU9056, in prostate cancer. *PLoS One* **7**, e45539 (2012).
12. Ghizzoni, M. *et al.* 6-alkylsalicylates are selective Tip60 inhibitors and target the acetyl-CoA binding site. *Eur. J. Med. Chem.* **47**, 337–344 (2012).
13. Dou, Z. *et al.* Dynamic localization of Mps1 to kinetochore is essential for accurate spindle microtubule attachment. *Proc. Natl. Acad. Sci. USA* **112**, E4546–E4555 (2015).
14. Ji, Z., Gao, H. & Yu, H. Kinetochore attachment sensed by competitive Mps1 and microtubule binding to Ndc80C. *Science* **348**, 1260–1264 (2015).
15. Hiruma, Y. *et al.* Competition between MPS1 and microtubules at kinetochores regulates spindle checkpoint signaling. *Science* **348**, 1264–1267 (2015).
16. Martin-Lluesma, S., Stucke, V.M. & Nigg, E.A. Role of Hec1 in spindle checkpoint signaling and kinetochore recruitment of Mad1/Mad2. *Science* **297**, 2267–2270 (2002).
17. Wood, K.W. *et al.* Antitumor activity of an allosteric inhibitor of centromere-associated protein-E. *Proc. Natl. Acad. Sci. USA* **107**, 5839–5844 (2010).
18. Carmena, M., Wheelock, M., Funabiki, H. & Earnshaw, W.C. The chromosomal passenger complex (CPC): from easy rider to the godfather of mitosis. *Nat. Rev. Mol. Cell Biol.* **13**, 789–803 (2012).
19. Lampson, M.A., Renduchitala, K., Khodjakov, A. & Kapoor, T.M. Correcting improper chromosome-spindle attachments during cell division. *Nat. Cell Biol.* **6**, 232–237 (2004).
20. Posch, M. *et al.* Sds22 regulates aurora B activity and microtubule-kinetochore interactions at mitosis. *J. Cell Biol.* **191**, 61–74 (2010).
21. Zeitlin, S.G., Shelby, R.D. & Sullivan, K.F. CENP-A is phosphorylated by Aurora B kinase and plays an unexpected role in completion of cytokinesis. *J. Cell Biol.* **155**, 1147–1157 (2001).
22. Yasui, Y. *et al.* Autophosphorylation of a newly identified site of Aurora-B is indispensable for cytokinesis. *J. Biol. Chem.* **279**, 12997–13003 (2004).
23. Sugiyama, K. *et al.* Aurora-B associated protein phosphatases as negative regulators of kinase activation. *Oncogene* **21**, 3103–3111 (2002).
24. Cohen, P., Klumpp, S. & Schelling, D.L. An improved procedure for identifying and quantitating protein phosphatases in mammalian tissues. *FEBS Lett.* **250**, 596–600 (1989).
25. Favre, B., Turowski, P. & Hemmings, B.A. Differential inhibition and posttranslational modification of protein phosphatase 1 and 2A in MCF7 cells treated with calyculin-A, okadaic acid, and tautomycin. *J. Biol. Chem.* **272**, 13856–13863 (1997).
26. Neumann, H., Peak-Chew, S.Y. & Chin, J.W. Genetically encoding N^{ε}-acetyllysine in recombinant proteins. *Nat. Chem. Biol.* **4**, 232–234 (2008).
27. Neumann, H. *et al.* A method for genetically installing site-specific acetylation in recombinant histones defines the effects of H3 K56 acetylation. *Mol. Cell* **36**, 153–163 (2009).
28. Honda, R., Körner, R. & Nigg, E.A. Exploring the functional interactions between Aurora B, INCENP, and survivin in mitosis. *Mol. Biol. Cell* **14**, 3325–3341 (2003).
29. Ruchaud, S., Carmena, M. & Earnshaw, W.C. Chromosomal passengers: conducting cell division. *Nat. Rev. Mol. Cell Biol.* **8**, 798–812 (2007).
30. Lemercier, C. *et al.* Tip60 acetyltransferase activity is controlled by phosphorylation. *J. Biol. Chem.* **278**, 4713–4718 (2003).
31. Charvet, C. *et al.* Phosphorylation of Tip60 by GSK-3 determines the induction of PUMA and apoptosis by p53. *Mol. Cell* **42**, 584–596 (2011).
32. Lin, S.Y. *et al.* GSK3-TIP60-ULK1 signaling pathway links growth factor deprivation to autophagy. *Science* **336**, 477–481 (2012).
33. Skoufias, D.A., Indorato, R.L., Lacroix, F., Panopoulos, A. & Margolis, R.L. Mitosis persists in the absence of Cdk1 activity when proteolysis or protein phosphatase activity is suppressed. *J. Cell Biol.* **179**, 671–685 (2007).
34. Foley, E.A. & Kapoor, T.M. Microtubule attachment and spindle assembly checkpoint signalling at the kinetochore. *Nat. Rev. Mol. Cell Biol.* **14**, 25–37 (2013).
35. Nijenhuis, W., Vallardi, G., Teixeira, A., Kops, G.J. & Saurin, A.T. Negative feedback at kinetochores underlies a responsive spindle checkpoint signal. *Nat. Cell Biol.* **16**, 1257–1264 (2014).
36. Holland, A.J. & Cleveland, D.W. Chromoanagenesis and cancer: mechanisms and consequences of localized, complex chromosomal rearrangements. *Nat. Med.* **18**, 1630–1638 (2012).
37. Kaidi, A. & Jackson, S.P. KAT5 tyrosine phosphorylation couples chromatin sensing to ATM signalling. *Nature* **498**, 70–74 (2013).
38. Nishino, T. *et al.* CENP-T-W-S-X forms a unique centromeric chromatin structure with a histone-like fold. *Cell* **148**, 487–501 (2012).
39. Tao, Y. *et al.* The structure of the FANCM-MHF complex reveals physical features for functional assembly. *Nat. Commun.* **3**, 782 (2012).
40. Janssen, A., van der Burg, M., Szuhai, K., Kops, G.J. & Medema, R.H. Chromosome segregation errors as a cause of DNA damage and structural chromosome aberrations. *Science* **333**, 1895–1898 (2011).
41. Xia, P. *et al.* EB1 acetylation by P300/CBP-associated factor (PCAF) ensures accurate kinetochore-microtubule interactions in mitosis. *Proc. Natl. Acad. Sci. USA* **109**, 16564–16569 (2012).
42. Xiao, Y. *et al.* Dynamic interactions between TIP60 and p300 regulate FOXP3 function through a structural switch defined by a single lysine on TIP60. *Cell Reports* **7**, 1471–1480 (2014).

Acknowledgments

We are grateful to Y. Shi (University of Science & Technology of China) and Y. Chen (Natural Science Foundation of China) for support; to S. Zhao (Fudan University) for mass spectrometric assistance; and to J. Chin (MRC Laboratory of Molecular Biology, Cambridge, UK) for reagents. This work was supported in part by the Natural Science Foundation of China (grants 31430054, 31320103904 and 91313303, 2002CB713700 to X.Y.; 31501095 to X.L.; 81270466 to X.D.; 31371363 to Z.D.; 31271439 to C.F.; and 91213303 to Z.W.), 973 projects (2014CB964803 to X.Y.; 2012CB917200 to J.Za., L.N.; 2012CB945002, 2013CB911203 to Z.D.; 2002CB713701 to C.F.); MOE Innovative team IRT13038, Fundamental Research Funds for the Central Universities WK2070000066; Chinese Academy of Sciences Center of Excellence 2015HSC-UE010; and the US National Institutes of Health (DK56292 and CA164133 to X.Y.).

Author contributions

X.Y. and G.F. conceived the project. F.M., X.Z. and X.L. designed and performed most biochemical and cell biological experiments. P.Y.Y., B.Q., Z.S., J.Za., Z.W. and J.Zh. performed chemical biological experiments and evaluated small molecule inhibitors. Z.D., C.T., M.T., L.N. and C.F. assisted in recombinant protein engineering and purification. F.M., X.Z., X.L., P.Y.Y., B.Q., Z.S., J.Za., C.F. and X.D. performed data analyses. F.M., X.Z., X.L. and X.Y. wrote the manuscript. D.L.H. and G.F. edited the manuscript.

Competing financial interests

The authors declare no competing financial interests.

Additional information

Any supplementary information, chemical compound information and source data are available in the online version of the paper. Reprints and permissions information is available online at http://www.nature.com/reprints/index.html. Correspondence and requests for materials should be addressed to X.Y.

ONLINE METHODS

Plasmids. Site-specific mutants of FLAG- or EGFP-tagged Aurora B and RNAi-resistant TIP60 were generated by PCR-based, site-directed mutagenesis kit from Vazyme (C212) according to the manufacturer's instructions. MBP (maltose-binding protein)–WT Aurora B and MBP–K215R Aurora B plasmids were generated by subcloning Aurora B from corresponding EGFP vectors into the pMal-c2 vector. The GST-H3 N-tail construct was obtained by cloning a PCR fragment corresponding to aa 1–15 of human histone H3 into the pGEX-6p1 vector. ACKRS3 and pCDF-pylT plasmids were gifts from the laboratory of J. Chin. pAB-HIS-INbox was constructed by inserting full-length Aurora B and a truncation of INCENP (aa 822–918) downstream of two adjacent T7 promoters in pCDF-pylT. The corresponding AAG codon in pAB-HIS-INbox was mutated to TAG in order to generate pAB-215TAG-HIS-INbox. All plasmids used were verified by sequencing (Invitrogen).

Cell culture, synchronization, and transfection. HEK293T and HeLa cells were purchased from the American Type Culture Collection and maintained as monolayers in advanced DMEM (Invitrogen) with 10% FCS (HyClone) and 100 units/mL of penicillin plus 100 μg/mL of streptomycin (Invitrogen). The cell lines used were not found in International Cell Line Authentication Committee (ICLAC) listings for cross-contaminated or otherwise misidentified cell lines. The cells were routinely tested for mycoplasma contamination. For cell cycle synchronization, HeLa cells were first blocked in G1/S with 2.5 mM thymidine (Sigma) for 16 h and then released in fresh culture medium for 8 h to enrich mitotic cells. Plasmid transfections were performed with Lipofectamine 2000 (Invitrogen) according to the manufacturer's instructions.

Inhibitors and treatments. Nocodazole (100 ng/mL, ≥99%), monastrol (50 μM, ≥98%), MG132 (10 μM, ≥90%), OA (500 nM, ≥92%), reversine (1 μM, ≥98%), roscovitine (20 μM, ≥98%), NAM (5 mM, ≥99.5%), and TSA (1 μM, ≥98%) were from Sigma. MG149 (100 μM, >99%) was from Axon. NU9056 (20 μM, >98%), ZM447439 (2 μM, >99%) were from Tocris Bioscience. GSK923295 (50 nM, >99%), BI2536 (100 nM, >99%), VX-680 (500 nM, >99%) was from Selleckchem. The protease inhibitors cocktail was from Sigma.

RNA interference. The lentivirus-based vector PLKO.1 along with pRSV-Rev, pMDLg/pRRE, and pMD2.G were ordered from Addgene and used for producing shRNA-packaged viral particles as previously described[43]. The nucleotide sequence for shRNA against TIP60 was 5′-CCTCCTATCCTATCGAAGCTA-3′ (#1) and 5′-TCGAATTGTTTGGGCACTGAT-3′ (#2). PLKO.1 vectors with shRNA containing scrambled sequence 5′-CCTAAGGTTAAGTCGCCCTCG-3′ were used to generate a control virus. Previously described siRNA duplexes were used to repress TIP60 (ref. 10), Mps1 (ref. 44), Nuf2 (ref. 45), Hec1 (ref. 46) and Aurora B[47]. 5′-UUCUCCGAACGUGUCACGUTT-3′ was used as a negative control siRNA. All siRNA duplexes were purchased from Qiagen and were transfected with Lipofectamine 2000 reagent (Invitrogen) according to the manufacturer's instructions.

Antibodies. Anti-TIP60 #1 (H-93, epitope aa 421–513, 1:1,000), anti-Mps1 (C-19, 1:1,000), and anti-Mad2 (17D10, 1:1,000) antibodies were from Santa Cruz. Anti-α-tubulin (ab80779, 1:5,000) was from Abcam. Anti-FLAG-tag (M2, 1:2,000) antibody was from Sigma. Anti-GST-tag (2625, 1:2,000), anti-His-tag (12698, 1:2,000), anti-HA-tag (3724,1:2,000), anti-MBP tag (2396, 1:2,000), anti-pS10-H3 (3377, 1:5,000), anti-RCC1 (5134, 1:1,000), anti-pS11-RCC1 Ser11 (5500, 1:1,000), anti-acetylated-lysine (9441, 1:1,000), and anti-pS7-CENP-A (2187, 1:1,000) antibodies were from Cell Signaling Technology. Anti-Aurora B (AIM-1, 1:2,000) antibody was from BD Biosciences. Anti-pT232-Aurora B antibody (600-401-677, 1:2,000) was from Rockland. Rabbit anti-TIP60 #2 (epitope aa 80–95, 1:1,000), anti-pS90-TIP60 (1:1,000) and anti–K215ac Aurora B (1:1,000) antibodies were generated by YenZym LLC. To generate anti-pS90-TIP60 antibody, a synthetic peptide containing phosphorylated S90 (*C*-KNGLPGSRPG-*p*S-PERE) was conjugated to rabbit albumin (Sigma) and injected into rabbits as previously described[48]. Serum was collected by a standard protocol and preabsorbed by unphosphorylated TIP60 peptide (*C*-KNGLPGSRPGSPERE) followed by affinity-purification using (*C*-KNGLPGSRPG-*p*S-PERE)-conjugated divinylsulfone Sepharose beads. Secondary antibodies were from Jackson ImmunoResearch Laboratory. To generate anti–K215ac Aurora B antibody, peptide containing acetylated K215 (GLKGEL-acK-IADFGWS; synthesized by YenZym) was conjugated to rabbit albumin (Sigma) and immunized into rabbits as previously described[48]. The serum was collected and preabsorbed by unacetylated Aurora B peptide (GLKGELKIADFGWS) followed by affinity-purification using (GLKGEL-acK-IADFGWS)-conjugated divinylsulfone Sepharose beads (Sigma).

Recombinant protein preparation. The acetylated protein was produced from *E. coli* as previously described[26,27]. Briefly, *E. coli* strain Rosetta (DE3) was transformed with pACKRS and pAB-215TAG-HIS-IN plasmids simultaneously. The bacteria were cultured in lysogeny broth medium supplemented with kanamycin (50 mg/mL) and spectinomycin (50 mg/mL) to OD_{600} of 0.7. Acetyl-lysine (AcK, 10 mM) and NAM (20 mM) were then added, the culture was incubated for 0.5 h, and protein expression was induced with IPTG (0.2 mM) at 37 °C for 4 h. The bacteria were lysed by sonication in Ni-NTA binding buffer (50 mM NaH_2PO_4, pH 8.0, 300 mM NaCl, 10 mM imidazole) and incubated with Ni-NTA agarose (Qiagen) for 1.5 h at 4 °C. The agarose was washed three times in Ni-NTA binding buffer supplemented with 20 mM imidazole and eluted with Ni-NTA binding buffer supplemented with 250 mM imidazole. The eluted protein was then dialyzed against dialysis buffer (25 mM Tris-HCl, pH 7.4; 100 mM NaCl; 10% glycerol) for 4 h at 4 °C.

GST-H3 (aa 1–15), MBP–WT Aurora B and MBP–K215R Aurora B were produced from bacteria as previously described[41]. Basically, the plasmids were transformed into *E. coli* strain Rosetta (DE3), and protein expression was induced with 0.2 mM IPTG at 16 °C. Bacteria expressing GST-H3 (aa 1–15) were suspended and lysed by sonication in PBS buffer supplemented with 1% Triton X-100. The preparation was incubated with glutathione-Sepharose 4B (GE Healthcare Life Science) for 1.5 h at 4 °C. The resin was washed three times, and GST-H3 protein was eluted with 10 mM glutathione. Bacteria expressing MBP–WT Aurora B and MBP–K215R Aurora were lysed in MBP column buffer (20 mM Tris-HCl, pH 7.4; 200 mM NaCl; 1 mM EDTA) and incubated with amylose resin (New England BioLabs) for 1.5 h at 4 °C. The resin was washed three times in MBP column buffer and eluted with MBP column buffer supplemented with 10 mM maltose. All purification procedures were performed at 4 °C, and protease inhibitor cocktail (Sigma) was added to prevent protein degradation.

Immunoprecipitation and pull-down assays. For immunoprecipitation, cells were treated with indicated reagents before being trypsinized and lysed in EBC buffer (50 mM Tris-HCl, pH 8.0; 120 mM NaCl; 0.5% NP-40) supplemented with protease inhibitor cocktail (Sigma), phosphatase inhibitor cocktail (Sigma), TSA (1 μM), and NAM (10 mM). After pre-clearing with protein A/G resin, the lysate was incubated with Aurora B antibody at 4 °C for 24 h with gentle rotation. Protein A/G resin was then added to the lysates, and they were incubated for another 6 h. The Protein A/G resin was then spun down and washed five times with lysis buffer before being resolved by SDS-PAGE and immunoblotted with the indicated antibodies. For FLAG-tagged protein immunoprecipitation, the FLAG-M2 resin was added to the lysates and incubated for 4 h before washing. For *in vitro* reactions, the FLAG-beads were further washed twice with dialysis buffer, and the FLAG-tagged protein was eluted with dialysis buffer supplemented with 100 μg/mL 3 × FLAG peptide (Sigma).

For pull-down assays, FLAG-PR65 was coexpressed with PP2A for 36 h and subjected to FLAG-M2 resin immunoprecipitation. The immunoprecipitated FLAG-PR65 was incubated with either wild-type Aurora B or K215ac Aurora B in EBC buffer supplemented with protease inhibitor cocktail (Sigma), phosphatase inhibitor cocktail (Sigma), TSA (1 μM), and NAM (10 mM). 4 h later, the binding fraction was washed with EBC buffer 5 times and analyzed by western blot.

Aurora B kinase assay and characterization of kinetics. Purified recombinant GST-H3 (1–15) and Aurora B were incubated in kinase buffer (25 mM HEPES, pH 7.4; 100 mM NaCl; 5 mM $MgCl_2$; 1 mM DTT) supplemented with 100 μM ATP and protease cocktail inhibitor for 20 min at 30 °C. The kinase reactions were stopped by addition of 5× Sample buffer (10% SDS; 0.5% bromophenol blue; 50% glycerol; 1 M DTT) before being resolved by SDS-PAGE and immunoblotted with indicated antibodies.

The kinetics of Aurora-B was characterized with Fluorometric Kinase Assay Kits (ATT Bioquest, 31001) following the manufacturer's instructions. Basically, Aurora B kinase was incubated with GST-histone H3 (1–15) in 20 μl kinetics assay buffer (60 mM HEPES, pH 7.5; 3 mM $MgCl_2$; 3 mM $MnCl_2$;

3 µM Na-orthovanadate) in the presence of 0–100 µM ATP for 0.5 h at 37 °C. Then the ADP sensor and sensor buffer were added, and the preparations were incubated for another 15 min at room temperature. The fluorescence intensities were monitored at Ex/Em = 540/590 nm to determine the formation of ADP. The reaction was repeated, and the K_m and k_{cat} values were calculated according to the Michaelis-Menten equation.

***In vitro* PP2A phosphatase assay.** Purified Aurora B was incubated with PP2A phosphatase (Millipore) in dephosphorylation buffer (50 mM Tris-HCl, pH7.4; 0.1 mM EDTA; 1 mM DTT; 2 mM $MgCl_2$; 0.01% Brij-35) in the presence of EDTA-free protease inhibitor cocktail (Roche) with gentle agitation. The reactions were stopped by addition of 5 × Sample buffer and heated at 95 °C for 5 min. The samples were resolved by SDS-PAGE and immunoblotted with indicated antibodies.

***In vitro* acetylation assay and characterization of TIP60 kinetics.** The acetylation reaction was performed essentially as previously described[41]. Basically, purified TIP60 was incubated with Aurora B in 30 µl HAT buffer (20 mM Tris-HCl, pH8.0; 10% glycerol; 100 mM NaCl; 1 mM DTT; 1 mM EDTA; 10 µM TSA; 10 mM NAM) containing 100 µM acetyl-CoA for 2 h at 37 °C. The reaction was stopped by addition of 5× Sample buffer and heated at 95 °C for 5 min before being resolved by SDS-PAGE and immunoblotted with indicated antibodies.

Methods for characterizing the acetyltransferase kinetics of TIP60 has been described[12]. Basically, purified TIP60 was incubated with H4 peptide (aa 1–20) and ^{14}C labeled Ac-CoA in 30 µl HAT buffer at 30 °C. After incubation, the mixture was loaded onto Waterman P81 filter paper and then washed with 50 mM of sodium bicarbonate (pH 9.0) for three times. The radioactive products were quantified by a liquid scintillation spectrometer. The reaction was repeated for three times, and the K_m and k_{cat} values were calculated according to the Michaelis-Menten equation.

Gel filtration assay. HeLa cells synchronized with nocodazole were lysed in EBC buffer (50 mM Tris-HCl, pH 8.0; 120 mM NaCl; 0.5% NP-40) supplemented with protease inhibitor cocktail (Sigma) and phosphatase inhibitor cocktail (Sigma). Lysates were then centrifuged for 30 min at 200,000*g*, and the supernatants were concentrated by Centriprep-10 (Millipore). Clarified lysates were filtered through a 0.45-µm membrane before being loaded onto a Superose 6, 10/300 GL column (GE Healthcare Life Sciences). Column fractions were then collected for SDS-PAGE and western blotting analyses.

Immunofluorescence and time-lapse imaging. HeLa cells grown on coverslips were fixed by a pre-extraction method using PTEM buffer (60 mM PIPES, pH 6.8; 10 mM EGTA; 2 mM $MgCl_2$; 0.2% Triton X-100) supplemented with 3.7% paraformaldehyde. After blocking with PBST (PBS with 0.05% Tween-20) buffer containing 1% bovine serum albumin (Sigma) for 45 min at room temperature, the fixed cells were incubated with primary antibodies in a humidified chamber for 1 h at room temperature or overnight at 4 °C, followed by secondary antibodies for 1 h at 37 °C. The DNA was stained with 4′,6-diamidino-2-phenylindole (DAPI) from Sigma. Images were captured by DeltaVision softWoRx software (Applied Precision) and processed by deconvolution and z-stack projection.

For Time-lapse imaging, HeLa cells were cultured in glass-bottom culture dishes (MatTek) and maintained in CO_2-independent media (Gibco) supplemented with 10% FBS and 2 mM glutamine[49]. During imaging, the dishes were placed in a sealed chamber at 37 °C. Images of living cells were taken with a DeltaVision microscopy system.

Fluorescence intensity quantification. Quantification of fluorescence intensity of kinetochore-associated proteins was performed as described previously using ImageJ[45]. In brief, the average pixel intensities from no less than five cells (which were randomly selected) were measured, and background pixel intensities were subtracted. The pixel intensities at each kinetochore pair were then normalized against ACA or Hec1 values to account for any variations in staining or image acquisition.

Statistics. All statistics were described in the figure legends. Two-sided unpaired Student's *t*-test was applied for experimental comparisons, using GraphPad Prism. All western blotting analyses were taken from three separated experiments. No statistical method was used to predetermine sample size. All data were expected to have normal distribution.

43. Moffat, J. *et al.* A lentiviral RNAi library for human and mouse genes applied to an arrayed viral high-content screen. *Cell* **124**, 1283–1298 (2006).
44. Dou, Z. *et al.* TTK kinase is essential for the centrosomal localization of TACC2. *FEBS Lett.* **572**, 51–56 (2004).
45. Liu, D. *et al.* Human NUF2 interacts with centromere-associated protein E and is essential for a stable spindle microtubule-kinetochore attachment. *J. Biol. Chem.* **282**, 21415–21424 (2007).
46. Chu, Y. *et al.* Aurora B kinase activation requires survivin priming phosphorylation by PLK1. *J. Mol. Cell Biol.* **3**, 260–267 (2011).
47. Yang, Y. *et al.* Phosphorylation of HsMis13 by Aurora B kinase is essential for assembly of functional kinetochore. *J. Biol. Chem.* **283**, 26726–26736 (2008).
48. Yao, X., Anderson, K.L. & Cleveland, D.W. The microtubule-dependent motor centromere-associated protein E (CENP-E) is an integral component of kinetochore corona fibers that link centromeres to spindle microtubules. *J. Cell Biol.* **139**, 435–447 (1997).
49. Ding, X. *et al.* Probing CENP-E function in chromosome dynamics using small molecule inhibitor syntelin. *Cell Res.* **20**, 1386–1389 (2010).

doi:10.1038/nchembio.2017